Proceedings of the 1st international Symposium on AI and Fluid Mechanics
Paper No S2 P4

# Fast personalized arterial flow inference with physics-informed neural networks and minimal non-invasive data

Sokratis J. Anagnostopoulos[1a], Georgios Rovas[a], Lydia Aslanidou[a],
George Em Karniadakis[b], Nikolaos Stergiopulos[a]

[a]*Laboratory of Hemodynamics and Cardiovascular Technology, EPFL, Lausanne, Switzerland*
[b]*Division of Applied Mathematics, Brown University, Providence, USA*

**Abstract**

Throughout the advancement of cardiovascular physiology, arterial flow models have been developed to study conditions such as stenoses and aneurysms, as well as to assess overall patient health. While conventional methods are valuable in clinical practice, they face limitations, particularly in personalized medicine. Physics-informed methods address these by integrating physical principles, reducing the need for extensive data. In this work, we develop an efficient physics-informed model which is able to infer the flow and pressure field within arterial bifurcations, given minimal non-invasive measurements of pressure. The model is based on our validated 1-D in-house code of the systemic arterial tree and trains in 3000 iterations, at least 10x faster than the current state-of-the-art models due to several model enhancements. We validate the model predictions against our 1-D solver, yielding a relative L2 error of $10^{-2}$, and perform additional tests for the patient-specific tuning of the terminal resistance and compliance during training, which are treated as learnable parameters with an error margin of $4 - 15\%$. The model learns the right personalized parameters on a laptop GPU within 10 minutes, holding promise towards applications of personalized cardiac output monitoring and hemodynamic assessment via wearable devices.

## 1. Introduction

The field of cardiovascular mechanics combines many different aspects of complex physics interactions: from non-Newtonian pulsating flow through an intricate system of vascular branching, to the non-linear visco-elasticity of the arterial wall and the interaction between the two. Our lab has focused on the 1-D modeling of the arterial network developing a generic 1-D model [1] and validating it against non-invasive measurements, offering valuable insights into flow and pressure waveforms across most vascular beds. The model encompasses systemic, coronary and cerebral arteries, along with heart dynamics and solves fluid mechanics equations numerically, incorporating a time-varying elastance model for the heart and considering systolic flow impediment in coronary arteries. It has been extensively used to investigate cardiovascular physiology, exploring the effects of arterial stiffening and aortic aneurysm reconstruction on wave reflections and central blood pressure [2, 3], and to provide patient-specific [4, 5] solutions. Moreover, it has been combined with advanced computational techniques like 3-D CFD and FSI to understand complex flow phenomena in the aorta and cerebral vasculature [6], and enabled the development and validation of non-invasive techniques for assessing vascular health [7, 8, 9].

Advances in Machine Learning (ML) are paving the way towards exploiting the information encapsulated in non-invasive, noisy biomedical measurements ranging from peripheral pressure data to Magnetic Resonance Imaging (MRI). These models are deployed in order to make fast and accurate predictions of important physiological indicators of the patient's cardiovascular health like the central arterial pressure [10], cardiac contractility [11], or the Wall Shear Stress field (WSS) [12]. A recent breakthrough in ML for physics were physics-informed neural networks (PINNs), which are not trained on just raw data

[1]email: sokratis.anagnostopoulos@epfl.ch

but also on the actual differential equations that govern the system (e.g. Navier-Stokes) [13, 14]. These networks have been previously applied on cardiovascular problems, either to make sense from noisy MRI data regarding the hemodynamics of the patient [15], or to recreate the full velocity, transient cuffless pressure or shear stress field from sparse measurements [16, 17]. PINNs have gained increased popularity due to their superiority in inverse problems, motivating researchers to develop methodologies to ease the optimization process.

This study investigates the application of an efficient PINN framework for the rapid solution of the PDEs governing the cardiovascular system, leveraging the validated arterial model developed at Laboratory of Hemodynamics and Cardiovascular Technology (LHTC). The proposed model enables the use of a single neural network to simultaneously compute the velocity, pressure, and area fields across various arterial segments. We demonstrate that accurate predictions of flow and pressure pulses within arterial bifurcations can be inferred using a single non-invasive pressure measurement at the radial artery. With the integration of PINN enhancements, the methodology provides patient-specific results in approximately 3000 iterations, with an error margin of 4-15%. In contrast, traditional inverse solution methods, which rely on multiple forward solutions with our 1-D numerical model, typically require several hours to compute.

## 2. Methods

### *2.1. 1-D arterial model*

Arteries are typically viewed as elongated, straight segments with a viscoelastic wall. The 1-D continuity and momentum equations (Navier-Stokes) are solved iteratively for an arterial network consisting of 103 conical segments, along with a constitutive law for the flexible arterial walls [1], described by the following closed-system of PDEs:

$$\frac{\partial Q}{\partial t} + \frac{\partial}{\partial x}\left(\int_A u^2 dA\right) = -\frac{A}{\rho}\frac{\partial P}{\partial x} - 2\pi R \frac{\mu}{\partial r}\bigg|_{r=R} + A f_x, \tag{1}$$

$$\frac{\partial P}{\partial t} = -\frac{1}{C_A}\left(\frac{\partial A}{\partial t} + \frac{\partial Q}{\partial x}\right), \tag{2}$$

$$\frac{\partial A}{\partial P} = \frac{A}{\rho \cdot PWV^2} \cdot \left[a + \frac{b}{1 + \left(\frac{P - P_{maxC}}{P_{width}}\right)^2}\right] = C_A, \tag{3}$$

where $A(x,t)$ is the arterial lumen area of radius $R(x,t)$, $Q(x,t)$ is the volumetric blood flow rate, $P(x,t)$ is the transmural pressure, $\mu$ is the blood viscocity, $f_x$ is the gravitational force, $P_{maxC}, P_{width}$ are constants, and $u(x,r,t)$ is the velocity profile approximated by the Witzig-Womersley theory. The constitutive law (Eq. 3), depends on the area compliance $C_A$, which is a function of arterial pulse wave velocity (PWV) and pressure. Finally, the conservation of mass and pressure is applied at the interface of each arterial bifurcation, while at the terminal arterial sites, a 3-element Windkessel model is used to simulate the omitted branches with their corresponding terminal resistance $R_T = R_1 + R_2$ and compliance $C_T$ parameters, which can be fine-tuned based on the patient, hence:

$$\frac{\partial Q}{\partial t} = \frac{1}{R_1}\frac{\partial P}{\partial t} + \frac{P}{R_1 R_2 C_T} + \left(1 + \frac{R_1}{R_2}\right)\frac{Q}{R_1 C_T}, \tag{4}$$

### *2.2. Physics-Informed Neural Networks (PINNs)*

In the context of PINNs, a general partial differential equation (PDE) can be expressed as:

$$\mathcal{D}\{u(x,t)\} = f(x,t), \tag{5}$$

where $u(x,t)$ is the unknown function we wish to approximate, $\mathcal{D}$ denotes the differential operator, and $f(x,t)$ is a given source or forcing function that introduces external influences to the system. The differential operator $\mathcal{D}$ depends on the specific PDE under consideration. Additionally, the problem may be constrained by several types of boundary conditions (e.g. Windkessel for terminal arteries).

The loss function $\mathcal{L}$ in PINNs is what drives the training process to the optimal state and is designed to encompass the deviation of the neural network prediction from the PDE solution and also the available measurements:

$$\mathcal{L} = \mathcal{L}_{IC} + \mathcal{L}_{BC} + \mathcal{L}_{\mathcal{R}} + \mathcal{L}_{data}, \tag{6}$$

where $\mathcal{L}_{IC}$, $\mathcal{L}_{BC}$ represent the residuals associated with the initial and boundary conditions of the problem, $\mathcal{L}_{\mathcal{R}}$ are the PDE residuals (calculated during training with automatic differentiation) and $\mathcal{L}_{data}$ is the deviation from the measured data. It is important to note that a conventional neural network would need a large dataset, as it is only trained using the term $\mathcal{L}_{data}$. On the other hand, PINNs exploit the known physics through the additional loss terms and require minimal measurements for the training process, which makes them ideal in a clinical setting where the available data may be scarce or noisy. Hence, they are designed to provide a seamless integration of the governing physical laws with the case-specific experimental data, representing a fast inverse solver.

Finally, each of these terms encourages the neural network to conform to the respective physical laws or initial/boundary conditions encoded in the problem. The training of the neural network weights is performed using a version of gradient descent (GD). In each iteration $k$, an update is applied to a network weight $w$ as follows:

$$w^{k+1} = w^k - \eta \cdot \nabla_w \mathcal{L}, \tag{7}$$

where $\eta$ is the learning rate, and $\nabla_w \mathcal{L}$ is the gradient of the loss function with respect to $w$. Each iteration updates the parameters $w$ iteratively, driving the solution towards satisfying the given PDE, measured data, boundary and initial conditions.

### *2.3. Inverse parameter estimation framework*

PINNs have been extensively used as efficient inverse solvers in the literature. The aim of this work is to apply a parametrized PINN model to estimate the personalized Windkessel parameters along with the cardiac output, given the carotid-to-femoral PWV (cfPWV) is known and a single pressure wave measurement is obtained at the end of the radial artery, as shown in the framework of Figure 1. The cfPWV is obtained via a one-time non-invasive measurement for each patient using a SphygmoCor (AtCor Medical) device, since it mainly varies with age, and the radial pressure pulse can be obtained by a pressure sensor or a wearable device placed on the wrist. For the purpose of the present study, we obtain these measurements directly from the 1-D solver, and perform an inverse solution using the PINN framework. More specifically, we start with a generic arterial tree as presented in our earlier study [1] and calculate the arterial distensibility parameter $\lambda_D$ which fits the cfPWV measurement from:

$$\text{cfPWV} = \frac{\sum_i L_i}{\sum_i L_i \sqrt{\rho \lambda_D \cdot D_i}}, \tag{8}$$

where $L_i, D_i$ is the length and diameter of each segment that lies in between, $\rho$ is the blood density, and $D_i$ is the distensibility of each segment. Next, using the calculated distensibility and an arbitrary flow pulse at the inlet (with adjusted heart rate (HR) based on the radial measurement period (T)), we perform a single forward solution to obtain an uncalibrated flow at the brachial inlet, which will serve as the initial condition for the PINN solver. The flow ($Q$), terminal compliance ($C_t$) and terminal resistance ($R_t$) parameters can be expressed as:

$$Q = \lambda_Q \cdot Q_0, \quad \mathbf{C_t} = \lambda_C \cdot \mathbf{C_{t0}}, \quad \mathbf{R_t} = \lambda_R \cdot \mathbf{R_{t0}}, \tag{9}$$

where $Q_0$ is the uncalibrated flow pulse, $\mathbf{C_{t0}}$ and $\mathbf{R_{t0}}$ are the vectors containing the corresponding compliance and resistances of all terminal arteries at initialization, and $\lambda_i$ are the trainable parameters to be estimated for a patient-specific solution.

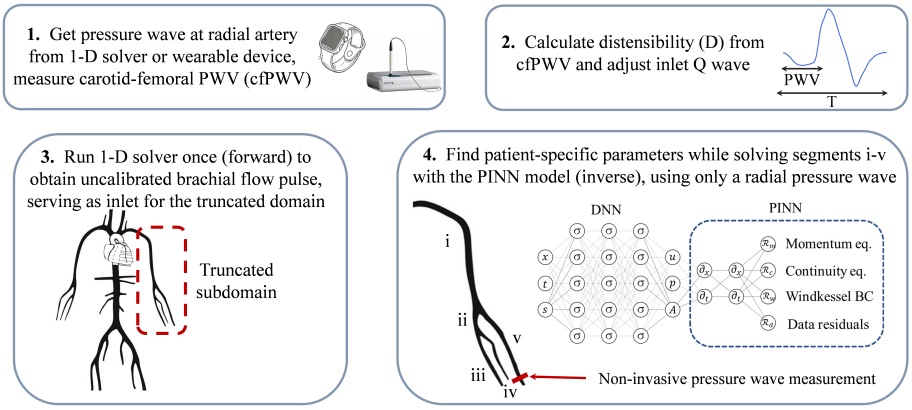


**Figure 1. Inverse solution framework:** The 1-D solver is used to produce an uncalibrated flow wave at the brachial inlet. The pressure wave measurement obtained at the radial artery is then fed into the PINN to infer the patient-specific parameters of the arterial tree, and provide an accurate flow and pressure prediction within the truncated arm geometry.

Finally, we train the neural network parameters including all three $\lambda$ using a two-stage optimization: 200 iterations with Rprop and 3000 iterations with LBFGS. The DNN architecture consists of 7 deep layers of 128 neurons each with 3 inputs, namely the position (x), time (t) and arterial segment (s). The latter input enables the inference of the solution fields within different arterial segments using the same parametrized-DNN. The performance of this approach is enhanced by expressing Eqs 1-4 with respect to the velocity (u), which is generally conserved with varying arterial diameter. We also note that all PDEs are normalized based on [18] to eliminate learning imbalances cased by dominant differential terms. Temporal periodicity is also enforced exactly using Fourier feature embeddings to transform the input vector [19]. The overall training time for obtaining a patient-specific solution is about 10 minutes on a personal laptop with an Nvidia 3060 GPU.

## 3. Results

### *3.1. Inverse solution prediction*

In this section, we present indicative flow fields produced by the PINN model, alongside the comparison between the numerical solution and the model predictions. In Figure 2, we plot the velocity (u), pressure (P) and area (A) fields for two of the five domains (brachial and radial arteries) as solved by the PINN model, while the dashed lines correspond to the positions of the velocity and pressure curves shown on the right. We note again that the PINN is trained using only the pressure wave at the outlet of the radial artery and the rest of the curves are shown for validation purposes. Our results show that the neural model is capable of producing a very accurate match for the flow pulses within the arterial tree, which also directly provides an accurate estimate of the cardiac output (CO). The pressure pulse at the outlet is also matched while at the inlet there is a disagreement on the timing of the reflected wave (at t=0.4). This discrepancy will be investigated in future versions as it could be attributed to the convergence criterion of either the neural model or the numerical solver. However, the reflection produced by the PINN looks qualitatively more reasonable timing-wise. An interesting observation is that in the inverse setting, the internal measurement at the radial artery contains information about both the forward and backward wave reflections. Thus, solving a truncated arterial tree as in our case, should in theory provide all the necessary information to obtain an accurate solution, even if major arterial segments (aorta, cerebral etc.) are omitted from the considered geometry.

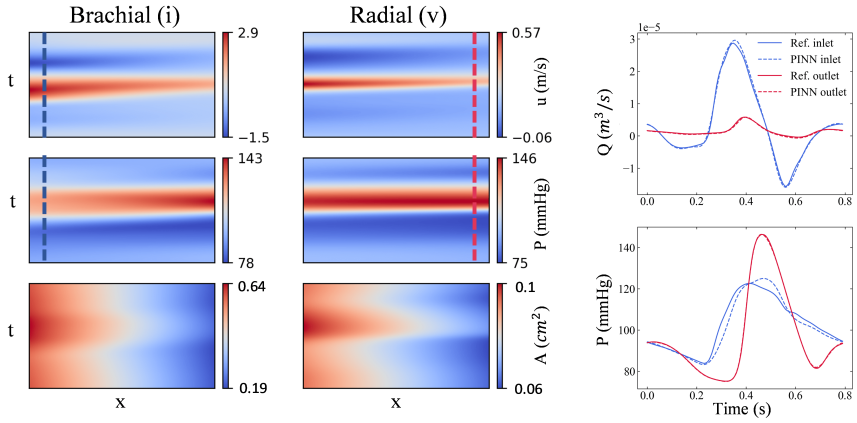


**Figure 2. PINN solution and comparison:** Indicative velocity (u), pressure (P) and the conical area (A) fields obtained by the PINN model (left). Comparison against the numerical solver on the dashed line positions (right).

### *3.2. Training convergence*

The optimization convergence is shown in Figure 3, where we plot both the loss (Eq. 6) and the relative L2 error, which represents the relative test loss given by:

$$\textit{Relative } L^2 = \frac{\|f(x;\theta) - u_e\|_2}{\|u_e\|_2}, \tag{10}$$

where $f(x;\theta)$ is the PINN prediction and $u_e$ is the reference solution (1-D solver). The convergence plots indicate that Rprop can be used as an efficient alternative primer for LBFGS, which often struggles to converge during the early learning stages. While Adam is usually applied prior to LBFGS, our experiments showed that it requires at least one order of magnitude more iterations on average than Rprop, hence we opted for the latter. Moreover, the temporal periodic boundary condition enables the network to converge within just one heart cycle, as opposed to $\sim$ 10 cycles that the numerical solver usually takes. The estimated parameters error for $[\lambda_Q, \lambda_{R_t}, \lambda_{C_t}]$ is [4%, 10%, 15%], which can be further improved with fine-tuning the model hyperparameters and constraining the search space of $\lambda$ based on physiological ranges. Notably, the computational time required is in the order of minutes compared to hours for a conventional inverse process using solely the 1-D solver and hundreds of forward solutions.

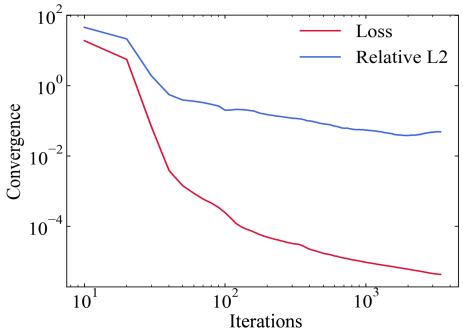


**Figure 3. Training convergence:** The full training takes roughly 3000 iterations: Rprop is used to warm up training for 200 iterations, followed by 3000 iterations of LBFGS. The converged solution takes approximately 10 minutes on a low-end GPU.

## 4. Summary

The present study explores the capabilities of an efficient PINN framework for the rapid solution of the PDEs governing the cardiovascular system, based on the validated arterial model developed at LHTC. Our model offers several attractive features: a) a single neural network can be used to obtain the velocity, pressure and area fields within different arterial segments for an arbitrary human arm geometry, b) the

flow and pressure pulses can be accurately predicted within arterial bifurcations and inferred at the inlet, c) the methodology and PINN enhancements produce patient-specific results in about 3000 iterations on average (about 10 minutes on a low-end GPU), with an error of 4-15%.

Future studies aim at further improving the accuracy of the patient-specific parameters by fine-tuning the network architecture and hyperparameters, but also via constraining the search space using physiological ranges. Moreover, we aim to test our model on a large dataset of real patients of varying age/height/weight, to evaluate its performance on the estimation of central clinical parameters like the central compliance (C), resistance (R), and the CO. Achieving reliable prediction on a clinical setting holds promise for simplifying health monitoring techniques and replacing current invasive approaches (e.g. using a pulmonary artery catheter) via non-invasive alternatives and wearable devices.

## References

[1] P. Reymond, F. Merenda, F. Perren, D. Rufenacht, N. Stergiopulos, Validation of a one-dimensional model of the systemic arterial tree, American Journal of Physiology-Heart and Circulatory Physiology 297 (1) (2009) H208–H222.

[2] P. Reymond, N. Westerhof, N. Stergiopulos, Systolic hypertension mechanisms: effect of global and local proximal aorta stiffening on pulse pressure, Annals of biomedical engineering 40 (2012) 742–749.

[3] O. Vardoulis, E. Coppens, B. Martin, P. Reymond, P. Tozzi, N. Stergiopulos, Impact of aortic grafts on arterial pressure: a computational fluid dynamics study, European Journal of Vascular and Endovascular Surgery 42 (5) (2011) 704–710.

[4] P. Reymond, Y. Bohraus, F. Perren, F. Lazeyras, N. Stergiopulos, Validation of a patient-specific one-dimensional model of the systemic arterial tree, American Journal of Physiology-Heart and Circulatory Physiology 301 (3) (2011) H1173–H1182.

[5] V. Bikia, S. Pagoulatou, B. Trachet, D. Soulis, A. D. Protogerou, T. G. Papaioannou, N. Stergiopulos, Noninvasive cardiac output and central systolic pressure from cuff-pressure and pulse wave velocity, IEEE journal of biomedical and health informatics 24 (7) (2019) 1968–1981.

[6] L. Augsburger, P. Reymond, D. Rufenacht, N. Stergiopulos, Intracranial stents being modeled as a porous medium: flow simulation in stented cerebral aneurysms, Annals of biomedical engineering 39 (2011) 850–863.

[7] T. G. Papaioannou, O. Vardoulis, N. Stergiopulos, The "systolic volume balance" method for the noninvasive estimation of cardiac output based on pressure wave analysis, American Journal of Physiology-Heart and Circulatory Physiology 302 (10) (2012) H2064–H2073.

[8] O. Vardoulis, T. G. Papaioannou, N. Stergiopulos, On the estimation of total arterial compliance from aortic pulse wave velocity, Annals of biomedical engineering 40 (2012) 2619–2626.

[9] T. G. Papaioannou, O. Vardoulis, A. Protogerou, G. Konstantonis, P. P. Sfikakis, C. Stefanadis, N. Stergiopulos, In vivo evaluation of a novel 'diastole-patching'algorithm for the estimation of pulse transit time: advancing the precision in pulse wave velocity measurement, Physiological measurement 36 (1) (2014) 149.

[10] H. Xiao, C. Liu, B. Zhang, Reconstruction of central arterial pressure waveform based on cnn-bilstm, Biomedical Signal Processing and Control 74 (2022) 103513.

[11] V. Bikia, T. G. Papaioannou, S. Pagoulatou, G. Rovas, E. Oikonomou, G. Siasos, D. Tousoulis, N. Stergiopulos, Noninvasive estimation of aortic hemodynamics and cardiac contractility using machine learning, Scientific reports 10 (1) (2020) 15015.

[12] B. Su, J.-M. Zhang, H. Zou, D. Ghista, T. T. Le, C. Chin, Generating wall shear stress for coronary artery in real-time using neural networks: Feasibility and initial results based on idealized models, Computers in biology and medicine 126 (2020) 104038.

[13] M. Raissi, P. Perdikaris, G. E. Karniadakis, Physics-informed neural networks: A deep learning framework for solving forward and inverse problems involving nonlinear partial differential equations, Journal of Computational physics 378 (2019) 686–707.

[14] L. Lu, X. Meng, Z. Mao, G. E. Karniadakis, Deepxde: A deep learning library for solving differential equations, SIAM review 63 (1) (2021) 208–228.

[15] G. Kissas, Y. Yang, E. Hwuang, W. R. Witschey, J. A. Detre, P. Perdikaris, Machine learning in cardiovascular flows modeling: Predicting arterial blood pressure from non-invasive 4d flow mri data using physics-informed neural networks, Computer Methods in Applied Mechanics and Engineering 358 (2020) 112623.

[16] K. Sel, A. Mohammadi, R. I. Pettigrew, R. Jafari, Physics-informed neural networks for modeling physiological time series for cuffless blood pressure estimation, npj Digital Medicine 6 (1) (2023) 110.

[17] A. Arzani, J.-X. Wang, R. M. D'Souza, Uncovering near-wall blood flow from sparse data with physics-informed neural networks, Physics of Fluids 33 (7) (2021).

[18] G. Kissas, Y. Yang, E. Hwuang, W. Witschey, J. Detre, P. Perdikaris, C. Team, et al., Machine learning in cardiovascular flows modeling: Predicting pulse wave propagation from non-invasive clinical measurements using physics-informed deep learning, in: APS Division of Fluid Dynamics Meeting Abstracts, 2019, pp. A31–001.

[19] S. Dong, N. Ni, A method for representing periodic functions and enforcing exactly periodic boundary conditions with deep neural networks, Journal of Computational Physics 435 (2021) 110242.